Brain Pathology ISSN 1015-6305

RESEARCH ARTICLE

Insights into the Infiltrative Behavior of Adamantinomatous Craniopharyngioma in a New Xenotransplant Mouse Model

Christina Stache[1]; Annett Hölsken[1]; Sven-Martin Schlaffer[2]; Andreas Hess[3]; Markus Metzler[4]; Benjamin Frey[5]; Rudolf Fahlbusch[6]; Jörg Flitsch[7]; Michael Buchfelder[2]; Rolf Buslei[1]

Departments of [1] Neuropathology, [2] Neurosurgery, [3] Pharmacology, [4] Pediatrics, [5] Radiation Oncology, Friedrich-Alexander-Universität Erlangen-Nürnberg, Erlangen; [6] International Neuroscience Institute, Hannover; [7] Department of Neurosurgery, University Hospital Hamburg-Eppendorf, Hamburg, Germany.

Keywords
craniopharyngioma, EGFR, invasivity, xenograft, β-catenin.

Corresponding author:
Rolf Buslei, MD, Department of Neuropathology, Friedrich-Alexander-Universität Erlangen-Nürnberg, Schwabachanlage 6, Erlangen 91054, Germany (E-mail: *rolf.buslei@uk-erlangen.de*)

Received 27 February 2014
Accepted 4 April 2014
Published Online Article Accepted 10 April 2014

Conflict of interest
The authors declare that they have no conflict of interest.

doi:10.1111/bpa.12148

Abstract

Adamantinomatous craniopharyngiomas (adaCP) cause hypothalamic pituitary dysfunction. Elucidation of pathomechanisms underlying tumor progression is essential for the development of targeted chemotherapeutic treatment options. In order to study the mechanisms of tumor outgrowth, we implanted human primary adaCP tissue from three different surgical specimens stereotactically into the brain of immunodeficient mice (n = 20). Three months after tumor inoculation, magnetic resonance imaging and histology confirmed tumor engraftment in all 20 mice (100%) that obtained tissue transplants. The lesions invaded adjoining brain tissue with micro finger-shaped protrusions. Immunohistochemical comparison of the primary tumor and xenotransplants revealed a similar amount of proliferation (Mib-1) and cytokeratin expression pattern (KL-1). Whole tumor reconstruction using serial sections confirmed whirl-like cell clusters with nuclear β-catenin accumulations at the tumor brain border. These whirls were surrounded by a belt of Claudin-1 expressing cells, showed an activated epidermal growth factor receptor (EGFR) and distinct CD133 as well as $p21^{WAF1/Cip1}$ positivity, indicating a tumor stem cell phenotype. Consistent with our previous *in vitro* studies, intracranial xenotransplants of adaCP confirmed cells with nuclear β-catenin and activated EGFR being the driving force of tumor outgrowth. This model provides the possibility to study *in vivo* tumor cell migration and to test novel treatment regimens targeting this tumor stem cell niche.

INTRODUCTION

Craniopharyngiomas (CP) are benign epithelial brain tumors which arise from embryonic remnants of Rathke's pouch epithelium (3). Approximately 2–5% of all primary intracranial neoplasms are adamantinomatous (adaCP) or papillary (papCP) CP (29). These subtypes have both histopathological differences as well as disparities in clinical manifestations and prognosis. Histomorphologically, the solid and homogenous papCP consists of well-differentiated squamous epithelium (10). As they generally present as well-circumscribed masses in suprasellar locations, once complete resection is achieved, tumor relapse is rare (1, 47). Although CP are histologically benign (World Health Organization Grade I) tumors, their anatomical proximity to crucial brain structures renders treatment procedures difficult and controversial (13, 15, 29, 33). Additionally, adaCP often form finger-shaped protrusions into the hypothalamus, the cavernous sinus and the visual system. AdaCP migration potential is enhanced by Wnt and epidermal growth factor receptor (EGFR) signaling (22, 23), which is activated in whirl-like cell clusters displaying distinct nuclear β-catenin accumulations. These clusters represent an alternatively differentiated cell population within the tumor bulk, showing the expression of different cytokeratins and tumor stem cell markers (9, 24). The complicated adaCP growth pattern makes total resection difficult to obtain without causing severe clinical and neuroendocrine deficits such as obesity, diabetes insipidus and pituitary hormone deficiencies (14, 34, 39, 40, 43). However, total resection is not excluded (15, 20). To reduce the chance of tumor relapse, subtotal resection is often accompanied by adjuvant radiotherapy; which can lead to treatment-associated side effects (29). Recent studies have reported additional chemotherapeutical approaches such as intracystic injection of bleomycin (45) and interferon-alpha (11, 12, 45). Because of small sample sizes and inadequate knowledge about their mechanisms of action, these medications do not represent "state of the art" treatment strategies. Presently, new targets for treatment strategies are exclusively based on studies performed *in vitro* and *ex vivo*, because an adequate *in vivo* model for this tumor entity has not yet been described. Recently, a genetically engineered adaCP animal model expressing a degradation-resistant mutant form of β-catenin in

early progenitor cells of Rathke's pouch was described. These mice developed sellar tumors with histological similarity to their human counterparts (19). This study confirmed the impact of deregulated Wnt/ β-catenin signaling in the pathogenesis of CP *in vivo* for the first time. Unfortunately, most animals did not survive weaning, making tumor growth studies over long time periods impossible. Two subcutaneous adaCP xenograft models have already been published before (7, 51) but orthotopic engraftment of tumor material is preferred because it better mimics original tumor morphology, special growth characteristics and environmental interactions. In addition, therapeutic response in orthotopic transplanted tumors correlates better with clinical outcomes, compared with subcutaneously transplanted tumor models (31). This applies particularly for brain tumors, where the blood–brain barrier forms a barricade for the effective delivery of several substances. Furthermore, it is known that direct implantation of fresh biopsy material is a better predictor of clinical outcomes than injection of tumor derived immortalized cell lines (18).

Here, we describe a reproducible intracranial xenograft model of human adaCP which allows analysis of the entire tumor growth pattern, as well as invasion of adjacent brain regions. Serial sections provided insights into tumor morphology as well as an overview of growth characteristics. Immunohistochemical characterization of whirl-like cell clusters at the invasion zone revealed the propulsive power of adaCP outgrowth.

MATERIALS AND METHODS

Patient collective

Fresh surgical specimens from three patients with adaCP were retrieved from the local Department of Neurosurgery. Instantaneous sections were prepared and microscopically reviewed to verify diagnosis and sufficient tumor content of each specimen (≥60%). Specimens were then divided for transplantation, cell culture and immunohistochemical analyses of the primary tumor. Each tumor sample was classified according to World Health Organization guidelines using hematoxylin and eosin (HE) as well as immunohistochemical stainings [e.g., pan-cytokeratin (KL-1) and β-catenin]. A declaration of consent of each patient is available for all specimens for further scientific investigation, approved by the local ethics committee of the Friedrich-Alexander-Universität Erlangen-Nürnberg. Procedures were conducted in accordance to the Declaration of Helsinki. Clinical data of all patients are presented in Table 1.

Immunohistochemistry

Surgical samples were prepared as described before (9). Immunohistochemical staining was performed using a staining machine (Benchmark XT; Ventana Roche, Illkirch, France) and the Ventana DAB staining system following the manufacturer's recommendations. The monoclonal mouse-antibody against cytokeratin-large-spectrum (1:40; clone KL-1; Beckman Coulter, Brea, CA, USA) was used to confirm epithelial differentiation. Proliferating cells were marked by a monoclonal rabbit-antibody against Mib-1 (1:200; Thermo Scientific, Waltham, MA, USA). For visualization of β-catenin, the monoclonal antibody mouse-anti-β-catenin (1:800; Clone 14; BD Biosciences, Franklin Lakes, NJ, USA) was applied. CD133 was detected with a polyclonal antibody generated in rabbit (1:20; Abnova, Taipei City, Taiwan). For staining of activated EGFR, we used a monoclonal rabbit-anti-EGFR-P antibody detecting the phosphorylated form of the receptor (1:250; clone EP774Y; Abcam, Cambridge, UK). Claudin-1 (CLDN1) was detected using a polyclonal rabbit-anti-Claudin-1 antibody (1:50; Cell Marque, Rocklin, CA, USA). To assess cell cycle arrest, we used a mouse-antibody against $p21^{WAF1/Cip1}$ (1:30; clone SX118; DAKO, Hamburg, Germany) (9).

Immunodeficient mouse models

We tested two different mouse strains for the generation of an adaCP xentotransplant model. The NMRI-$Fox1^{nu}$/$Fox1^{nu}$ (Janvier Elevage, Le Genest St. Ile, France) is a mutant mouse model characterized by thymic aplasia. Because of the lack of the thymus, thymus-dependent T-cell response is largely impaired (38). Innate immunity is not affected and NK-cell activity is still present. The Jackson Laboratory recently developed the profoundly immunodeficient mouse strain of NSG (NOD.Cg-*Prkdc*^{scid} *Il2rg*^{tm1Wjl}/SzJ). NSG lacks mature T- and B-cells as well as NK-cells and exhibit additional deficiencies in innate immunity because of a defective IL-2 receptor gamma chain (35). The absence of an adaptive immune response is explained by their inability to rearrange antigen receptors (VDJ recombination) (32). Comparing different NOD/SCID mouse strains revealed a superior engraftment of human cells in NSG mice (26). We used outbred male and female mice with an age of 5–8 weeks when brought into the experimental procedure.

Animal husbandry

All animals are housed in the local center for animal experiments (Franz-Penzoldt-Zentrum, University Hospital Erlangen, Erlangen, Germany). The center maintains standardized housing conditions as well as hygiene management according to the guidelines of the European Federation for Laboratory Animal Science Associations. The animals are kept under special pathogen-free conditions with autoclaved environment and indi-

Table 1. Summary of clinical data of patients included in this study and invasiveness of respective xenografts.
Abbreviations: adaCP = adamantinomatous craniopharyngioma; *CTNNB1* = β-catenin gene.

CP	Sex	Age	*CTNNB1* mutations	Clinically invasive	Mice (n)	Protrusions (n)
adaCP 1	Female	16	32/GAC (Asp) > AAC (Asn)	Invasive	4	4
adaCP 2	Male	45	36+37/deletion	Not invasive	8	4
adaCP 3	Male	40	33/TCT (Ser) > TGT (Cys)	Invasive	8	3

vidually ventilated cages with filtered air. Athymic nude mice require a higher temperature (25°C) and higher humidity (65%), maintained by an enclosed airflow cabinet (Ehret Bioscape, Uni Protect, Emmendingen, Germany). Handling of all animals was performed under a hood with laminar-airflow only. An accommodation time of 14 days was met to adapt all animals to the new environment prior to the beginning of experimental procedures. All animals were kept in a 12/12 h light-dark cycle with free access to sterilized, acidified drinking water (pH 2.5–2.8) and gamma-irradiated feed *ad libitum*. The experiments performed in this study were authorized by the local government (Regierung von Mittelfranken, Germany) in accordance with the animal protection act.

Transplantation procedure

Mice were anesthetized with 0.12 mg/gBW ketamine in combination with 0.016 mg/gBW xylazine i.p. The head of the mouse was fixed in a stereotactical frame (Bilaney Consultants, Düsseldorf, Germany) with blunt ear bars to avoid injuring of the eardrum. Efficacy of the anesthesia was tested by stimulating the thin skin between the toes with forceps. To avoid hypothermia, the animals were kept on a heating plate until awakening. After disinfection of the scalp, a 5 mm long incision was made anteriorly, in the direction of the interaural line. A burr hole with a diameter of 1 mm was drilled 3 mm lateral to the bregma. Through this hole, the mouse obtained uncultivated tumor tissue from surgical specimens. We aimed to transplant 1–8 mm^3 of solid tumor tissue with a sterile cannula. Control mice received only a 3 μL phosphate buffered saline injection with a Hamilton syringe. Afterwards, the skin was closed with a suture (ETHILON*II 4-0, Ethicon, Norderstedt, Germany). For pain relief, the animals received 1 mg/g metamizole (Ratiopharm, Ulm, Germany) with the drinking water 3 days following the procedures. Health condition of all animals was monitored daily by controlling body weight and monitoring for behavioral changes.

Magnetic resonance imaging (MRI)

To ensure tumor engraftment, MRI (1.5 Tesla Magnetom, Siemens Medical Systems, Erlangen, Germany) of the rodent's brain was conducted. Mice were anesthetized with 0.12 mg/gBW ketamine in combination with 0.016 mg/gBW xylazine. For better visualization of xenografts, all mice received an i.p. injection of contrast agent (Gadovist® 1 mmol/ml, Bayer, Leverkusen, Germany). We used a small flex loop surface RF-coil to visualize rodent's brain structures according to the protocol of Brockmann *et al* with T1- and T2-weighted sequences (6). Imaging took about 15 minutes per mouse, during which the animals were kept on a heating plate to avoid hypothermia. Performing MRI at 4.7 Tesla (BioSpec 47/40, Bruker, Billerica, MA, USA) allowed high resolution imaging. It is important to scan at a high spatial resolution in order to obtain a sufficient geometric description of the tumor. Therefore, a FISP sequence was used with following parameterization: FOV: 22 mm × 22 mm × 11 mm, matrix 256 × 256 × 128, coronal slices, TE 6.1 ms, TR 12.3 ms, alpha 15 degree, bandwidth 50 kHz and 30 averages providing 87 μm isotropic resolution. Mice were anesthetized with permanent delivery of isoflurane for the scan time which lasts about 1 h 50 minutes.

Sacrifice and preparation of immunohistochemistry

The animals were anesthetized and sacrificed by decapitating after MRI. Brains were dissected and fixed in 4% paraformaldehyde for further histological analyses. Paraffin-embedded serial sections of the mouse brain were analyzed histologically to reveal tumor morphology.

RESULTS

Imaging and histology revealed tumor engraftment in all tumor-transplanted mice

Three months after tumor transplantation, we conducted 1.5 Tesla MRI to screen the rodent's brains for tumor engraftment. The T1-weighted MR sequences revealed clearly visible, mostly contrast-enhancing lesions with a volume of 1 to 20 mm^3 in all mice that obtained tumor tissue before. Some tumors showed low signal intensity in the center of the lesion surrounded by a signal-rich zone at the lesion-brain interface. High resolution MRI performed at 4.7 Tesla enabled 3D reconstruction of a subset of xenografts, illustrating a typical CP growth pattern with micro finger-shaped tumor protrusions into adjacent brain areas (Figure 1A) in accordance with histological processing (Figure 1B). Engraftment of fresh surgical tumor specimens reached a tumorigenic efficacy of 100%. We revealed no differences in tumor engraftment between the two different mouse strains we tested. HE stainings of paraffin embedded mice brains showed epithelial tumors centered in the subdural space, but penetrating into surrounding brain parenchyma, sometimes reaching hippocampal and ventricular structures (n = 11; Figure 2A). Morphologically, the tumor grafts revealed clear parallels to the human counterparts (Figure 2B). They were characterized by the presence of epithelial cells arranged in lobules bordered by a palisaded columnar epithelium. In eight out of 20 cases, regressive elements such as pseudo-microcystical loosening, calcifications and nodules of wet keratin were predominant.

All xenografts showed a typical bordering zone between tumor tissue and the surrounding brain. This area, marked by a distinct gliosis and appearance of undifferentiated neuroepithelial cells, was similar to that seen in human adaCP (8). Even the growth behavior was comparable between the primary tumor and the xenograft model. Therefore, HE staining revealed an expansion into the rodent's brain similar to the infiltrative growth pattern in humans (Figure 3). In contrast, a solid and well-demarcated primary tumor developed in a xenograft counterpart in nearly the same way (not shown). The transplants showed an average cell proliferation similar to that observed in primary tumors, proving vitality 3 months after transplantation (Figure 3; Mib-1). Moreover, we detected cell clusters with a cell cycle arrest, assessed by $p21^{WAF1/Cip1}$ positivity, which is a typical tumor stem cell-like characteristic (Figure 3; $p21^{WAF1/Cip1}$). Tumor engraftment was seen irrespectively of the β-catenin mutation status and age of the donor patients. Given that we initially transplanted only three different human primary CP samples, this conclusion has to be confirmed in further studies. No control mouse showed any solid tumor growth within the brain; only hemosiderin deposits and hypoxic cells near the puncture channel were detectable (not shown).

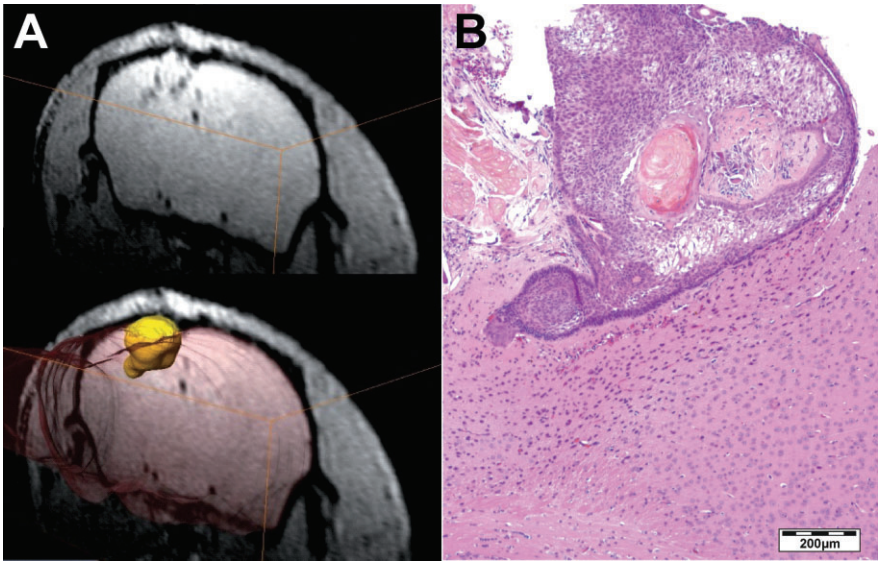

Figure 1. Three months after tumor transplantation 4.7 Tesla magnetic resonance imaging revealed subdural located lesions. The T1-weighted sequences enabled 3D-reconstruction of xenotransplants to comprehend the development of finger-shaped tumor protrusions into subjacent brain tissue (**A**). Hematoxylin and eosin staining of the corresponding histologically processed xenotransplant confirms the extrusive growth pattern (**B**).

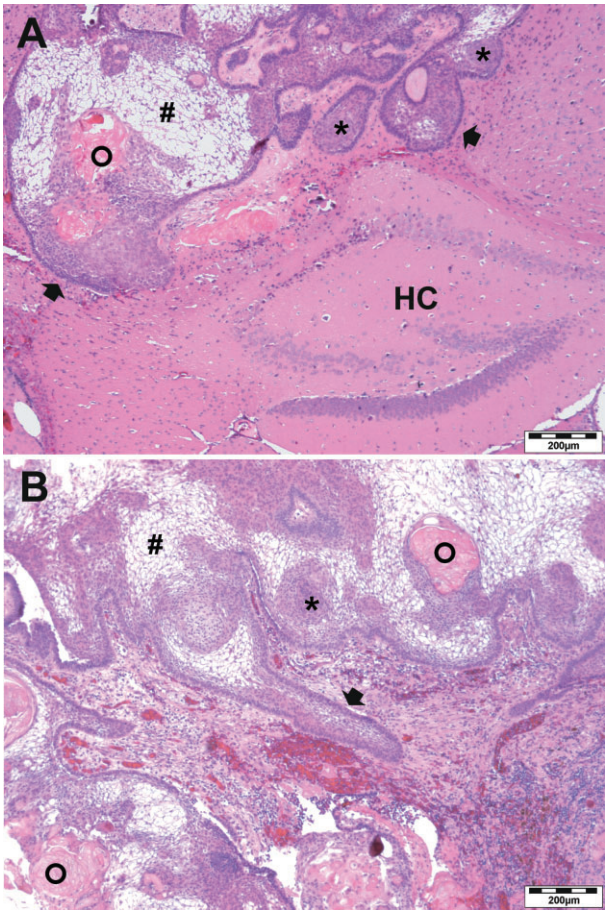

Figure 2. Xenografts touched the hippocampus (HC) and showed all histological hallmarks of adaCP in a hematoxylin and eosin staining. The basal cell layer (arrow) circumscribes epithelial lobular cell nests (asterisks) and regressive elements. Pseudo-microcystical loosening (rhombs) and wet keratin (circles) are present in the xenotransplants (**A**) as well as in the corresponding primary human tumor (**B**).

Formation of micro finger-shaped tumor protrusions into the surrounding brain tissue can be demonstrated using serial sections

Nine out of 20 xenografts showed distinct finger-shaped tumor protrusions within the surrounding brain, whereas two more tumors showed slight protuberance into adjacent structures (Table 1). To reconstruct the process of tumor outgrowth and to examine the cells being involved in this process step by step, we conducted extensive reprocessing of a whole xenotransplant in serial sections (Figure 4). Here, disordered tumor cell clusters from the tumor bulk overgrow the bordering basal cell layer of palisaded cells to promote tumor outgrowth. Figure 4, section 1 shows a clearly demarcated tumor with an intact basal cell layer. In further sections, a protuberance of tumor cells develops (arrow in 3). Subsequent sections reveal the formation of a finger-shaped tumor protrusion surrounded by an intact basal cell layer [4–5]. In the following sections, the outer cell layer is no longer bordering the tumor, but whirl-like configured tumor cells press forward into the central nervous tissue [6–9]. In this stage of tumor outgrowth, the basal cell layer is completely missing and the tumor outgrowth initiating cells get in direct contact with the extracellular matrix. Subsequently, the bordering cell layer regenerates and encloses these clusters, which than build whirls within the tumor bulk [10–11]. This process repeats at multiple sites of the tumor [12–18] and represents the mechanism of adaCP tumor branching. The involved cell clusters, characterized in detail in the succeeding sections, showed enhanced migratory potential and represent the driving force of adaCP outgrowth.

Infiltrating tumor cell clusters showed nuclear β-catenin accumulations, activated EGFR and expression of tumor stem cell marker CD133

To further characterize and compare human tumors with corresponding xenografts, we performed immunohistochemistry using a panel of antibodies (Figure 5). The major part of tumor cells

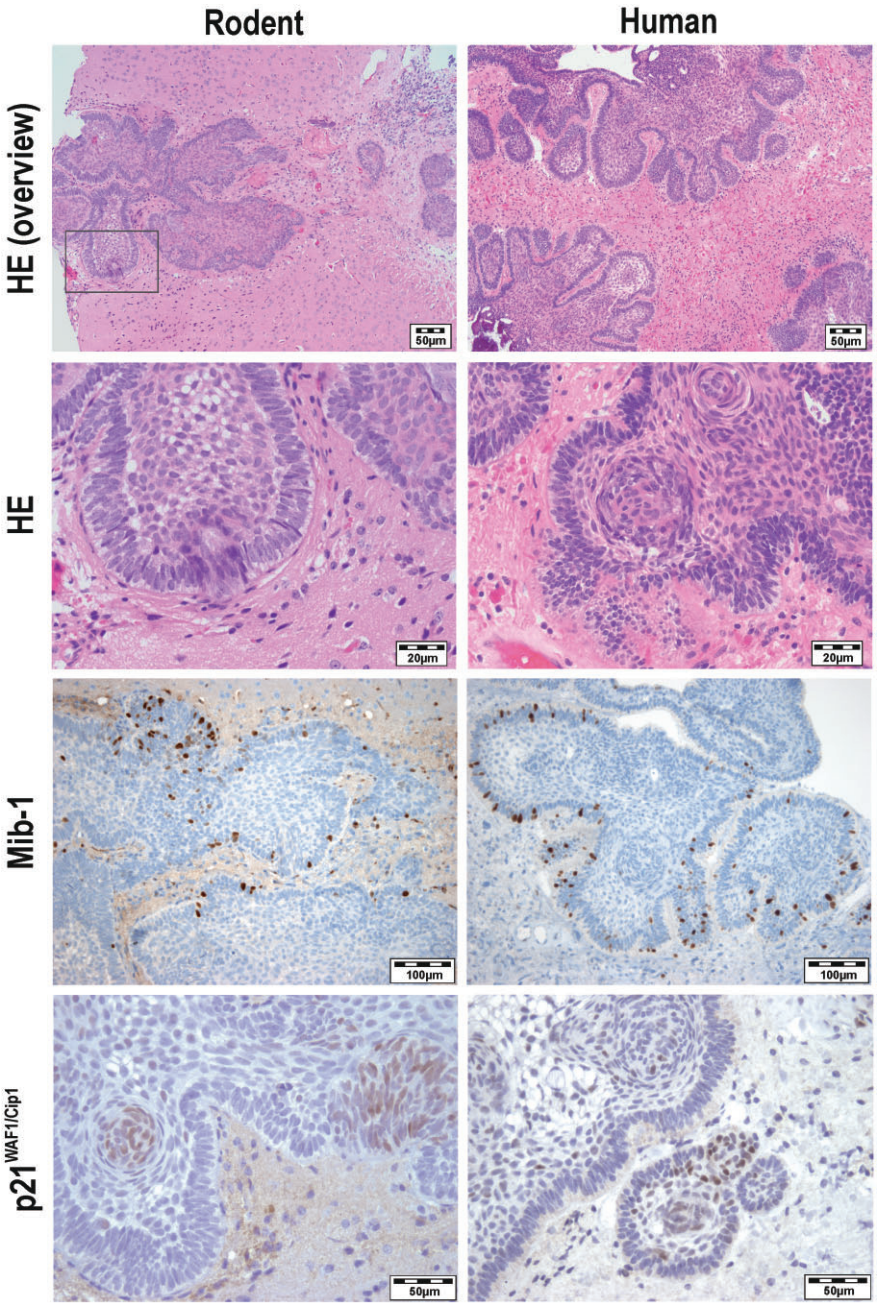

Figure 3. Histological reprocessing of the xenografts (Rodent) and comparison with the primary tumor (Human) showed a similar growth pattern. Overview of hematoxylin and eosin staining (HE) illustrates branched, invasive tumor growth into the rodent's brain. Whereas whirl-like configured cell formations even overcome the basal cell layer to promote tumor outgrowth. Proliferation activity indicated by expression of Mib–1 was also similar between primary tumor and xenograft. Primary and rodent tumors exhibit quiescent cell clusters indicated by expression of $p21^{WAF1/Cip1}$.

showed a homogenous and distinct staining with an antibody against pan-cytokeratin (KL-1), proving their epithelial differentiation. In contrast, whirl-like tumor cell clusters partially overgrowing the basal cell layer did not express Mib-1 (not shown) and obviously less KL-1, but showed nuclear β-catenin accumulations and enhanced membranous expression of CD133. Phosphorylated and, therefore, activated EGFR was expressed within the entire xenograft. However, cell clusters positive for nuclear β-catenin showed a shift from a purely membranous staining to a distinct cytoplasmic and nuclear appearance of phosphorylated EGFR. As described recently for human samples, these cell clusters were circumscribed by a belt of CLDN1-expressing cells, whereas the rest of the tumor appeared almost CLDN1 negative (44).

DISCUSSION

The problem in CP therapy is the lack of appropriate chemotherapeutical approaches targeting their infiltrative growth pattern, interspersing vital brain structures of crucial importance. We have previously shown that β-catenin accumulating cell clusters with activated EGFR are responsible for adaCP tumor cell migration. These cells are often arranged in whirls within the tumor matrix

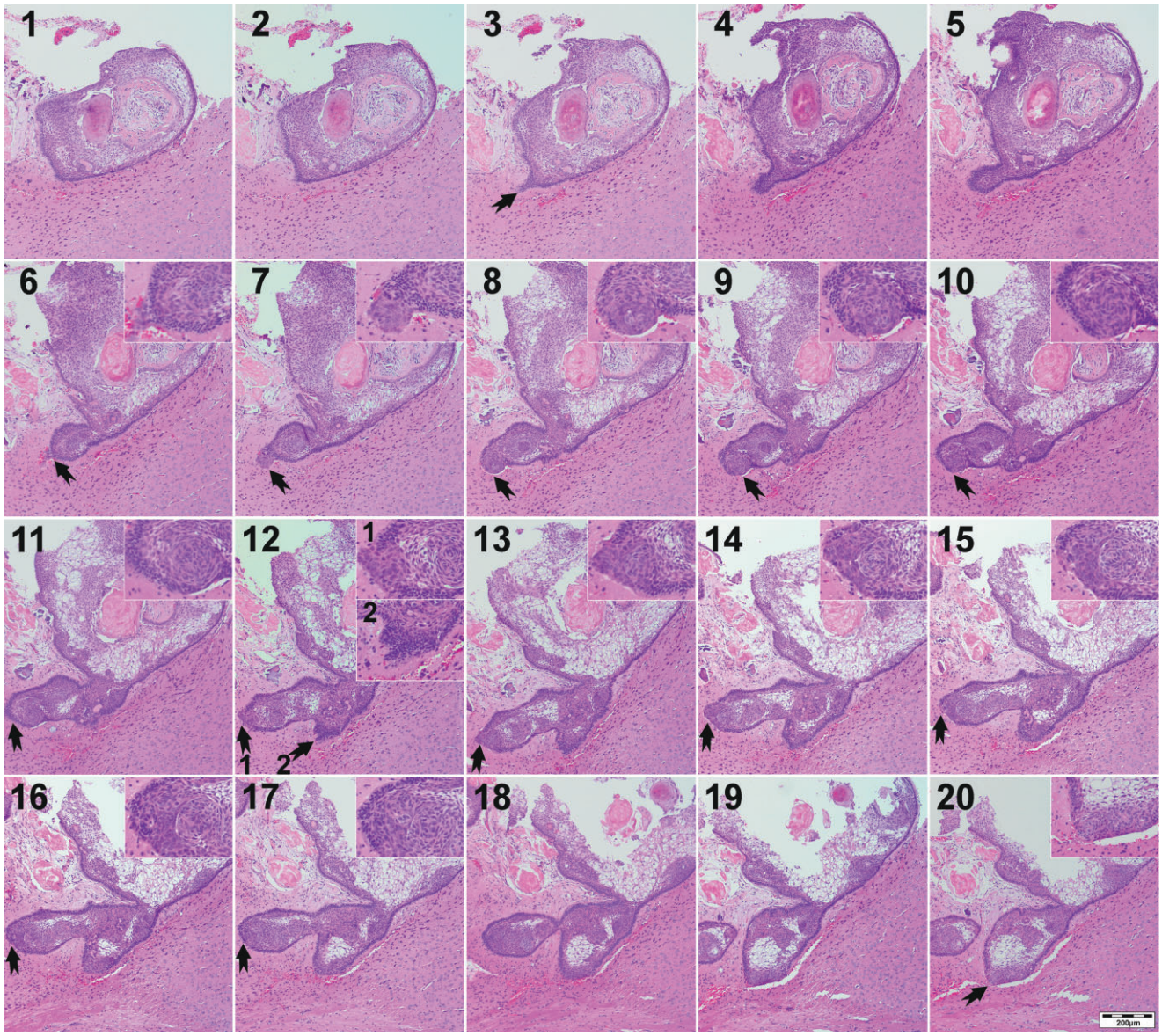

Figure 4. Serial sections of a whole xenograft illustrate the development of finger-shaped tumor protrusions (arrows) into adjacent central nervous tissue. The tumor forms a protuberance digging deeper into the brain [3–5] whereas the initially intact basal cell layer breaks up [6] when whirl-like, dedifferentiated tumor cells extrude [7]. The cell clusters are in direct contact then with the environment before the basal cell layer encloses the formation again [11]. This procedure recurs at multiple sites of the xenograft [arrows in 12] and seems to be the driving force of CP outgrowth and characteristical finger-shaped tumor protrusions. Enlarged inserts show the crucial sites (arrows).

and in areas of finger-shaped tumor protrusions. They represent an alternatively differentiated population of potential tumor stem cells (9, 23, 24). The β-catenin accumulating cells within the whirl-like structures may comprise cells that invade the brain either in a cell-autonomous manner or they may direct other cells non-cell autonomously by secretion of cytokines (3, 4). The suggestion that these cells may promote tumor cell migration, and therefore represent the propulsive power of adaCP outgrowth is difficult to ascertain from human tumor samples. In surgical specimens the tumor bulk is almost always disrupted, rendering the entire morphology difficult to assess. Histological slices only provide a snapshot in time of the outgrowing tumor areas. The rupture of the basal cell layer in human tumor samples can, therefore, only be seen by chance if the specimen contains surrounding brain tissue, which is often not included, in order to preserve crucial neuronal structures (21). Moreover, in small biopsies, whirl-like tumor cell clusters appear seldom or are entirely absent. One explanation for this observation is the fact that the areas of investigational interest are often located at the brain–tumor border and because of cautious resection this area is often not removed.

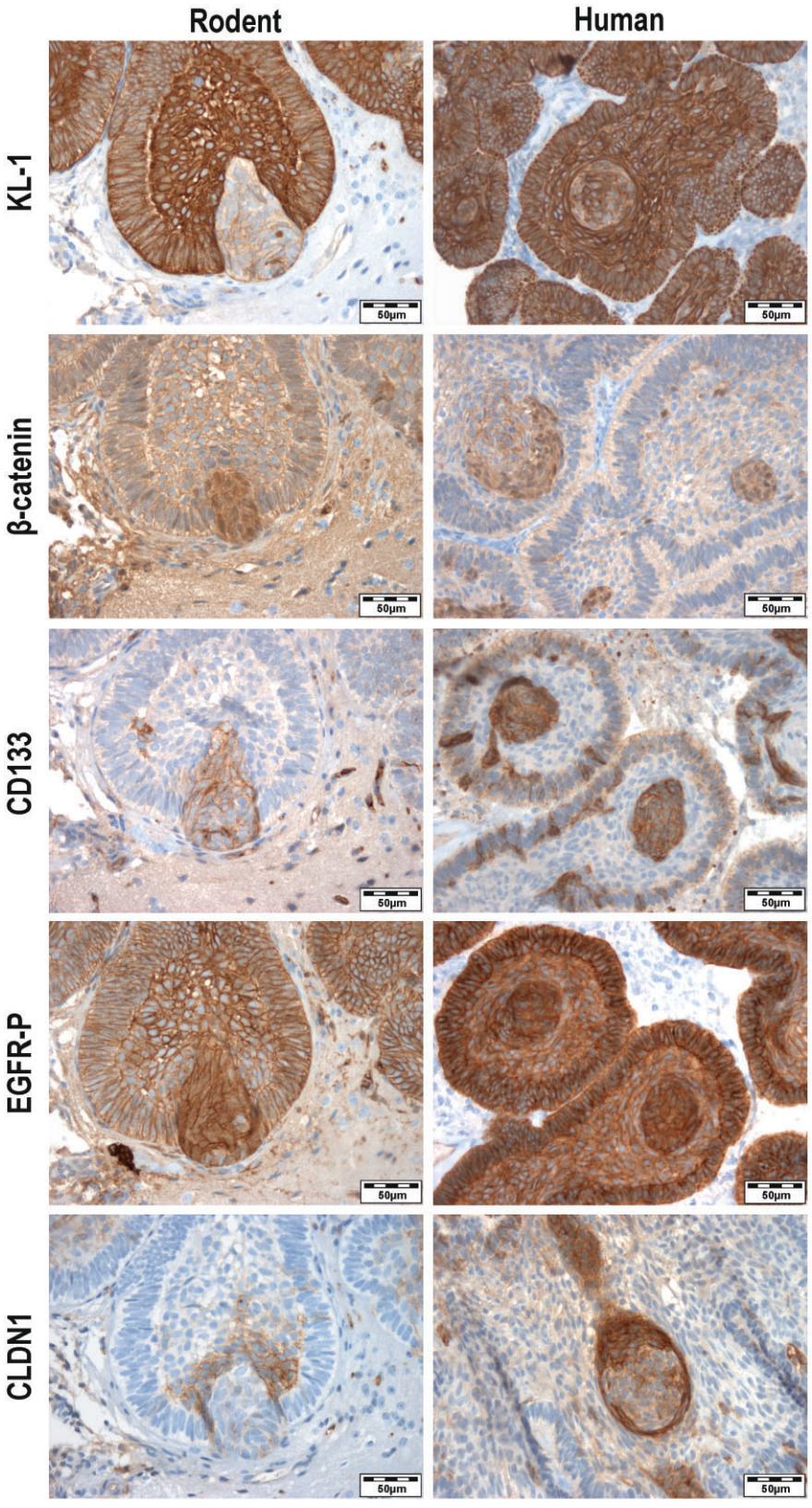

Figure 5. The xenografts (Rodent) showed accordance with the primary tumor (Human) concerning the expression of important immunohistochemical markers to characterize adaCP. The epithelial differentiation was proved by distinct expression of the pan-cytokeratin marker KL-1. Interestingly, within the xenografts and the primary tumors whirl-like cell clusters with nuclear accumulation of β-catenin and activated EGFR (EGFR-P) break through the basal cell layer and show less KL-1 expression, indicating dedifferentiation. Furthermore, these cells exhibit strong expression of the stem cell marker CD133 which further supports the hypothesis of a tumor stem cell phenotype. The whirls are surrounded by a belt of CLDN1 expressing cells, but lack the expression of this cell adhesion molecule themselves. Abbreviations: adaCP = adamantinomatous craniopharyngioma; CLDN1 = Claudin-1.

For the first time, this xenograft model presented herein allows reconstruction of the whole tumor bulk and characterization of the cells initiating tumor outgrowth.

We were able to show that primary tumor specimens of adaCP are tumorigenic and able to build intracranial tumors in immune suppressed mice resembling their human counterparts. Comparison of xenografts and donor tumors revealed analogous growth patterns, for example, cyst formation, extent of regressive changes and tendencies to infiltrate surrounding tissue. This was independent of the β-catenin mutation status and patients age. These histological features are distinctive characteristics of adaCP. We could detect a clearly concordant histological pattern while comparing the donor tumor samples and the xenotransplants. Therefore, we are convinced that regressive changes and microcystical loosening were not generated *de novo* in the mice. The xenograft model allows survival and promotes infiltration of the tumor tissue. We did not expect the tumors to gain mass extensively during the 3 months under study, because adaCP are generally designated as benign lesions with relatively low proliferation indices. A precise statement concerning real tumor growth can only be given if tumor size is monitored directly after transplantation and before sacrifice. The presented cases showed only moderate and comparable proliferation rates within human tumors and xenografts. As common chemotherapeutical approaches mostly target proliferating tumor cells, these substances are not indicated in CP therapy. The clinically more relevant task affecting the surrounding brain structures is the peculiar finger-shaped outgrowth of adaCP which can be examined here in detail. In serial sections of whole mice brains, we were able to show the process of tumor branching step by step. Thereby, whirl-like cell clusters showing nuclear β-catenin accumulations and activated EGFR are not only located within the tumor bulk, but overgrow the basal cell layer at many sites of the lesion, infiltrating the adjoining nervous tissue. This reflects the initiating step of tumor branching in adaCP, as epithelial differentiation (KL-1), cell adhesion (CLDN1) as well as proliferation (Mib-1) within the cell clusters are diminished. Accordingly, $p21^{WAF1/Cip1}$ is enhanced in the same cell clusters, indicating that these cells underwent a cell cycle arrest (9). The distinct expression of membranous CD133 led to the assumption that these alternatively differentiated cells probably represent a tumor stem cell population. The existence of proliferation-inhibited, migrating stem cells (41, 50) was already shown in solid tumors (28, 37). Cells that show the expression of tumor stem cell markers including CD133 and CD44, described in whirl-like cell clusters of adaCP (24), are known to be less sensitive to radiotherapy, therefore, causing tumor recurrence (5, 36, 46). The enhanced expression of $p21^{WAF1/Cip1}$ was also related to radioresistance in tumor cells (30). Priming these potential tumor stem cell niches by using chemotherapeutics may lead to a better response to radiotherapy in CP treatment, to reduce long-term tumor recurrence. Therefore, it is indispensable to investigate CP growth at the orthotopic site of tumor origin. As we have shown earlier, adaCP generate a tumor-specific cellular environment at the brain invasion border (8). The surrounding conditions within the brain cannot be mimicked in a subcutaneous xenograft model, underlining the importance of an intracranial *in vivo* CP model. The impaired immune system makes the nude mouse an optimal host for engraftment of xenotransplants (17, 42). Fiebig *et al* established xenografts of a wide set of human tumor specimens in immunodeficient mice. Further, they could prove accordance of the xenograft's response to therapeutical agents compared with the response in respective patients in 90% (16). Despite immunodeficiency, the nude mouse displays a robust animal model, drop outs or problems concerning health conditions occur rarely when handled carefully. NSG mice are more sensitive especially concerning anesthesia, for which reason they must be handled more delicately. As we observed no difference in tumor engraftment rates, we emphasize to perform further studies with $NMRI^{nu/nu}$-mice.

Our xenograft model represents a reasonable addition to a recently presented transgenic mouse model, which confirms the hypothesis that activated Wnt signaling is a key player in the development of adaCP (19). This study identified precisely that adaCP arise from progenitor cells of Rathke's pouch epithelium. Further investigations of these cells have identified several pathways that may be involved in tumor progression, which could be inhibited using small-molecule inhibitors (3). Therefore, xenotransplants generated with human adaCP in immunosuppressed mice offer another level of testing diverse new drugs and treatment options closer to the patients. We focused on xenografts established from adaCP because this subtype is much more difficult to treat in case of infiltrative tumor growth. PapCP appear well demarcated and are, therefore, often completely resectable with a lower risk of tumor recurrence compared with adaCP patients (1, 47). Further treatment strategies, that can be tested now *in vivo*, should focus on these cells displaying a tumor stem cell phenotype. Tumor cell migration is required for adaCP brain invasion, which was shown to be directly affected by Wnt and EGFR signaling. Inhibition of EGFR using the tyrosine kinase inhibitor, Gefitinib (Iressa®, Astra Zeneca, London, UK), displayed a promising target-specific treatment option for CP *in vitro* (22). This xenotransplantation model allows future *in vivo* administration of various tyrosine kinase inhibitors. Furthermore, other promising approaches as application of interferon-alpha (11, 25, 27) can be studied using this model. Interferon-alpha deserves further investigation as it has been shown to induce apoptosis of tumor cells (25, 49), and nuclear export of β-catenin (48). Furthermore, an additive effect in combination with Gefitinib (2, 52) was already shown to impede tumor progression.

In summary, we present the first intracranial xenograft model for human adaCP. Examination of whole tumor transplants in serial sections revealed whirl-like cell clusters with activated Wnt and EGFR signaling pathways as the propulsive power of tumor outgrowth, therefore, displaying targets for future treatment strategies.

ACKNOWLEDGMENTS

The study was funded by the Internationale Stiftung Neurobionik. We are indebted to Tajana Jungbauer and Diana Maron for performing immunohistochemical stainings. We express our special thanks to Trevor Steve (MD) for revising the manuscript.

REFERENCES

1. Adamson TE, Wiestler OD, Kleihues P, Yasargil MG (1990) Correlation of clinical and pathological features in surgically treated craniopharyngiomas. *J Neurosurg* **73**:12–17.

2. Amato RJ, Jac J, Hernandez-McClain J (2008) Interferon-alpha in combination with either imatinib (Gleevec) or gefitinib (Iressa) in metastatic renal cell carcinoma: a phase II trial. *Anticancer Drugs* **19**:527–533.
3. Andoniadou CL, Gaston-Massuet C, Reddy R, Schneider RP, Blasco MA, Le Tissier P *et al* (2012) Identification of novel pathways involved in the pathogenesis of human adamantinomatous craniopharyngioma. *Acta Neuropathol* **124**:259–271.
4. Andoniadou CL, Matsushima D, Mousavy Gharavy SN, Signore M, Mackintosh AI, Schaeffer M *et al* (2013) Sox2(+) stem/progenitor cells in the adult mouse pituitary support organ homeostasis and have tumor-inducing potential. *Cell Stem Cell* **13**:433–445.
5. Baumann M, Krause M, Hill R (2008) Exploring the role of cancer stem cells in radioresistance. *Nat Rev Cancer* **8**:545–554.
6. Brockmann MA, Ulmer S, Leppert J, Nadrowitz R, Wuestenberg R, Nolte I *et al* (2006) Analysis of mouse brain using a clinical 1.5 T scanner and a standard small loop surface coil. *Brain Res* **1068**:138–142.
7. Bullard DE, Bigner DD (1979) Heterotransplantation of human craniopharyngiomas in athymic "nude" mice. *Neurosurgery* **4**:308–314.
8. Burghaus S, Holsken A, Buchfelder M, Fahlbusch R, Riederer BM, Hans V *et al* (2010) A tumor-specific cellular environment at the brain invasion border of adamantinomatous craniopharyngiomas. *Virchows Arch* **456**:287–300.
9. Buslei R, Holsken A, Hofmann B, Kreutzer J, Siebzehnrubl F, Hans V *et al* (2007) Nuclear beta-catenin accumulation associates with epithelial morphogenesis in craniopharyngiomas. *Acta Neuropathol* **113**:585–590.
10. Buslei R, Nolde M, Hofmann B, Meissner S, Eyupoglu IY, Siebzehnrubl F *et al* (2005) Common mutations of beta-catenin in adamantinomatous craniopharyngiomas but not in other tumours originating from the sellar region. *Acta Neuropathol* **109**:589–597.
11. Cavalheiro S, Di Rocco C, Valenzuela S, Dastoli PA, Tamburrini G, Massimi L *et al* (2010) Craniopharyngiomas: intratumoral chemotherapy with interferon-alpha: a multicenter preliminary study with 60 cases. *Neurosurg Focus* **28**:E12.
12. Cohen M, Bartels U, Branson H, Kulkarni AV, Hamilton J (2013) Trends in treatment and outcomes of pediatric craniopharyngioma, 1975–2011. *Neuro-Oncol* **15**:767–774.
13. Crowley R, Hamnvik O, O'Sullivan E, Behan L, Smith D, Agha A, Thompson C (2010) Morbidity and mortality in craniopharyngioma patients after surgery. *Clin Endocrinol (Oxf)* **73**:516–521.
14. Elowe-Gruau E, Beltrand J, Brauner R, Pinto G, Samara-Boustani D, Thalassinos C *et al* (2013) Childhood craniopharyngioma: hypothalamus-sparing surgery decreases the risk of obesity. *J Clin Endocrinol Metab* **98**:2376–2382.
15. Fahlbusch R, Hofmann BM (2008) Surgical management of giant craniopharyngiomas. *Acta Neurochir (Wien)* **150**:1213–1226.
16. Fiebig HH, Maier A, Burger AM (2004) Clonogenic assay with established human tumour xenografts: correlation of in vitro to in vivo activity as a basis for anticancer drug discovery. *Eur J Cancer* **40**:802–820.
17. Flanagan SP (1966) "Nude", a new hairless gene with pleiotropic effects in the mouse. *Genet Res* **8**:295–309.
18. Garber K (2009) From human to mouse and back: "tumorgraft" models surge in popularity. *J Natl Cancer Inst* **101**:6–8.
19. Gaston-Massuet C, Andoniadou CL, Signore M, Jayakody SA, Charolidi N, Kyeyune R *et al* (2011) Increased Wingless (Wnt) signaling in pituitary progenitor/stem cells gives rise to pituitary tumors in mice and humans. *Proc Natl Acad Sci USA* **108**:11482–11487.
20. Hofmann BM, Hollig A, Strauss C, Buslei R, Buchfelder M, Fahlbusch R (2012) Results after treatment of craniopharyngiomas: further experiences with 73 patients since 1997. *J Neurosurg* **116**:373–384.
21. Holsken A, Buchfelder M, Fahlbusch R, Blumcke I, Buslei R (2010) Tumour cell migration in adamantinomatous craniopharyngiomas is promoted by activated Wnt-signalling. *Acta Neuropathol* **119**:631–639.
22. Holsken A, Gebhardt M, Buchfelder M, Fahlbusch R, Blumcke I, Buslei R (2011) EGFR signaling regulates tumor cell migration in craniopharyngiomas. *Clin Cancer Res* **17**:4367–4377.
23. Holsken A, Kreutzer J, Hofmann BM, Hans V, Oppel F, Buchfelder M *et al* (2009) Target gene activation of the Wnt signaling pathway in nuclear beta-catenin accumulating cells of adamantinomatous craniopharyngiomas. *Brain Pathol* **19**:357–364.
24. Holsken A, Stache C, Schlaffer SM, Flitsch J, Fahlbusch R, Buchfelder M, Buslei R (2013) Adamantinomatous craniopharyngiomas express tumor stem cell markers in cells with activated Wnt signaling: further evidence for the existence of a tumor stem cell niche? *Pituitary* [Epub ahead of print].
25. Ierardi DF, Fernandes MJ, Silva IR, Thomazini-Gouveia J, Silva NS, Dastoli P *et al* (2007) Apoptosis in alpha interferon (IFN-alpha) intratumoral chemotherapy for cystic craniopharyngiomas. *Child's Nerv Syst* **23**:1041–1046.
26. Ito M, Hiramatsu H, Kobayashi K, Suzue K, Kawahata M, Hioki K *et al* (2002) NOD/SCID/gamma(c)(null) mouse: an excellent recipient mouse model for engraftment of human cells. *Blood* **100**:3175–3182.
27. Jakacki RI, Cohen BH, Jamison C, Mathews VP, Arenson E, Longee DC *et al* (2000) Phase II evaluation of interferon-alpha-2a for progressive or recurrent craniopharyngiomas. *J Neurosurg* **92**:255–260.
28. Jung A, Brabletz T, Kirchner T (2006) The migrating cancer stem cells model–a conceptual explanation of malignant tumour progression. *Ernst Schering Found Symp Proc* (5):109–124.
29. Karavitaki N, Cudlip S, Adams CB, Wass JA (2006) Craniopharyngiomas. *Endocr Rev* **27**:371–397.
30. Kokunai T, Tamaki N (1999) Relationship between expression of p21WAF1/CIP1 and radioresistance in human gliomas. *Jpn J Cancer Res* **90**:638–646.
31. Kuo TH, Kubota T, Watanabe M, Furukawa T, Kase S, Tanino H *et al* (1993) Site-specific chemosensitivity of human small-cell lung carcinoma growing orthotopically compared to subcutaneously in SCID mice: the importance of orthotopic models to obtain relevant drug evaluation data. *Anticancer Res* **13**:627–630.
32. Malynn BA, Blackwell TK, Fulop GM, Rathbun GA, Furley AJ, Ferrier P *et al* (1988) The scid defect affects the final step of the immunoglobulin VDJ recombinase mechanism. *Cell* **54**:453–460.
33. Muller HL (2012) Craniopharyngioma—a childhood and adult disease with challenging characteristics. *Front Endocrinol* **3**:80.
34. Muller HL, Gebhardt U, Teske C, Faldum A, Zwiener I, Warmuth-Metz M *et al* (2011) Post-operative hypothalamic lesions and obesity in childhood craniopharyngioma: results of the multinational prospective trial KRANIOPHARYNGEOM 2000 after 3-year follow-up. *Eur J Endocrinol* **165**:17–24.
35. Ohbo K, Suda T, Hashiyama M, Mantani A, Ikebe M, Miyakawa K *et al* (1996) Modulation of hematopoiesis in mice with a truncated mutant of the interleukin-2 receptor gamma chain. *Blood* **87**:956–967.
36. Pajonk F, Vlashi E, McBride WH (2010) Radiation resistance of cancer stem cells: the 4 R's of radiobiology revisited. *Stem Cells* **28**:639–648.

37. Park J, Kim JM, Park JK, Huang S, Kwak SY, Ryu KA *et al* (2014) Association of p21-activated kinase (PAK)-1 activity with aggressive tumor behavior and poor prognosis of head and neck cancer. *Head Neck* [Epub ahead of print].
38. Pelleitier M, Montplaisir S (1975) The nude mouse: a model of deficient T-cell function. *Methods Achiev Exp Pathol* **7**:149–166.
39. Pierre-Kahn A, Recassens C, Pinto G, Thalassinos C, Chokron S, Soubervielle JC *et al* (2005) Social and psycho-intellectual outcome following radical removal of craniopharyngiomas in childhood. A prospective series. *Child's Nerv Syst* **21**:817–824.
40. Reschke K, Busse S, Mohnike K, Buchfelder M, Ranke M, Fahlbusch R, Lehnert H (2006) [CranioNet—an interdisciplinary strategy for craniopharyngioma]. *German Medical Weekly* **131**:821–824.
41. Romanov VS, Pospelov VA, Pospelova TV (2012) Cyclin-dependent kinase inhibitor p21(Waf1): contemporary view on its role in senescence and oncogenesis. *Biochemistry (Mosc)* **77**:575–584.
42. Rygaard J (1969) Immunobiology of the mouse mutant "Nude". Preliminary investigations. *Acta Pathol Microbiol Scand* **77**:761–762.
43. Sainte-Rose C, Puget S, Wray A, Zerah M, Grill J, Brauner R *et al* (2005) Craniopharyngioma: the pendulum of surgical management. *Child's Nerv Syst* **21**:691–695.
44. Stache C, Holsken A, Fahlbusch R, Flitsch J, Schlaffer SM, Buchfelder M, Buslei R (2014) Tight junction protein claudin-1 is differentially expressed in craniopharyngioma subtypes and indicates invasive tumor growth. *Neuro-Oncol* **16**:256–264.
45. Steinbok P, Hukin J (2010) Intracystic treatments for craniopharyngioma. *Neurosurg Focus* **28**:E13.
46. Sun M, Zhou W, Zhang YY, Wang DL, Wu XL (2013) CD44 gastric cancer cells with stemness properties are chemoradioresistant and highly invasive. *Oncol Lett* **5**:1793–1798.
47. Szeifert GT, Sipos L, Horvath M, Sarker MH, Major O, Salomvary B *et al* (1993) Pathological characteristics of surgically removed craniopharyngiomas: analysis of 131 cases. *Acta Neurochir (Wien)* **124**:139–143.
48. Thompson MD, Dar MJ, Monga SP (2011) Pegylated interferon alpha targets Wnt signaling by inducing nuclear export of beta-catenin. *J Hepatol* **54**:506–512.
49. Thyrell L, Arulampalam V, Hjortsberg L, Farnebo M, Grander D, Pokrovskaja Tamm K (2007) Interferon alpha induces cell death through interference with interleukin 6 signaling and inhibition of STAT3 activity. *Exp Cell Res* **313**:4015–4024.
50. Whale A, Hashim FN, Fram S, Jones GE, Wells CM (2011) Signalling to cancer cell invasion through PAK family kinases. *Front Biosci (Landmark Ed)* **16**:849–864.
51. Xu J, You C, Zhang S, Huang S, Cai B, Wu Z, Li H (2006) Angiogenesis and cell proliferation in human craniopharyngioma xenografts in nude mice. *J Neurosurg* **105**(Suppl. 4): 306–310.
52. Yang JL, Qu XJ, Russell PJ, Goldstein D (2005) Interferon-alpha promotes the anti-proliferative effect of gefitinib (ZD 1839) on human colon cancer cell lines. *Oncology* **69**:224–238.